REE-bearing minerals in the albitites of central Sardinia, Italy

G. Carcangiu, M. Palomba and M. Tamanini

Centro Studi Geominerari e Mineralurgici del C.N.R., Fac. di Ingegneria, Università di Cagliari, 09123 Cagliari, Italy

Abstract

Recent studies on albitite rocks located in the granodiorite complex of Central Sardinia have revealed that epidote has a widespread occurrence as a light rare-earth element (*LREE*)-bearing accessory common phase. Titanite has been recorded as a heavy rare earth element (*HREE*)-bearing mineral. The Hercynian granodiorite complex of Central Sardinia is composed chiefly of quartz, Ca-plagioclase, K-feldspar and biotite and of a wide variety of secondary assemblages, mainly allanite, titanite and zircon. Albitic plagioclase and quartz are the main mineral components of the albitites. Additional minerals include, besides allanite and epidote, a more calcic-plagioclase (oligoclase), K-feldspar, chlorite, titanite and more rarely muscovite. The mineral assemblages and *REE*-bearing minerals of albitites were analysed by wavelength dispersive spectrometry (WDS). Chemical data suggest that there is a near complete solid-solution between epidote and allanite whereas little variations in *HREE* of titanites were detected. In epidote-group minerals a pronounced zoning in *REE* was observed while titanite was recorded unzoned. Textural relations were studied by SEM to distinguish primary from secondary epidotes. Chemical criteria to recognize magmatic from alteration epidotes were also applied. The alteration epidotes mainly occur and generally originate from plagioclase alteration and from leaching of magmatic allanite. Comparison of textures using both the SEM technique and EPMA data showed that the characteristic 'patchy zoning', observed in epidotes, corresponds with different amounts of *REE* in these minerals.

The schematic model proposed for the epidote-forming reactions during the metasomatic processes that affected the granodiorites involves: (i) the instability of the anorthitic component of plagioclase; (ii) the simultaneous formation of albite; (iii) the leaching of the magmatic allanite with a redistribution of *REE* in the epidotes of the albitites.

Keywords: rare earth elements, albitite rocks, Sardinia, epidote, allanite, titanite.

Introduction

Several albitite deposits outcropping over an area of about 90 km^2 in the Ottana-Sarule-Orani-Oniferi sector (central Sardinia) and hosted within the Hercynian granitoid complex were recently investigated to ascertain the occurrence and consistency of *REE* mineralization (Bornioli *et al.*, 1993). Accessory minerals (mainly allanite) of granitoids contain a high proportion of whole-rock *REE*. Although they are normally immobile during the alteration processes, the nature of the original *REE*-bearing mineral phases, composition of the fluid phase, presence of ligands in solution (F, Cl and CO_2) and ability of newly-formed minerals to accommodate *REE* from the fluid, may enhance the *REE* mobility. The *REE* have been mobilized during the later Hercynian metasomatic alteration affecting the granodiorites of the investigated area (Carcangiu *et al.*, 1993).

This paper deals with the mineralogy of the albitites, the *REE* content and their distribution in the *REE*-bearing minerals, and suggests a schematic model for the epidote-forming reactions during metasomatic processes that affected the granodiorites.

Geological setting

The geological setting of the investigated area is schematized in Fig. 1. The basement of north-central

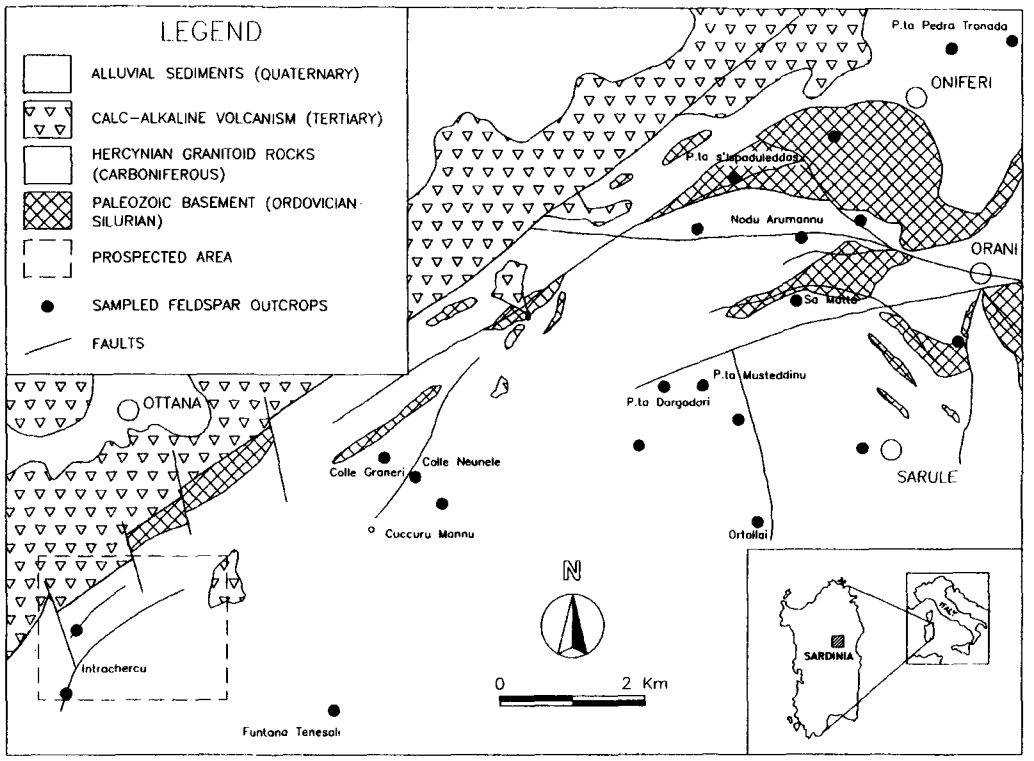

FIG. 1. Geological map of the investigated area and location of sampling areas.

Sardinia consists of volcanic and sedimentary sequences, tectonized and metamorphosed during the Hercynian orogeny and invaded by large amounts of late- and post-tectonic Hercynian granitoids (Elter *et al.*, 1986). The schistosity is associated with the deformation phases and the metamorphic recrystallization frequently obliterates the character of the precursor rocks. The tectonic-metamorphic events developed in Sardinia in the time span 350–300 Ma and the metamorphism is generally of medium-low grade. Although stratigraphic reconstruction of Palaeozoic metamorphic formations of central Sardinia has not yet been made (Elter *et al.*, 1986), in the investigated area, shales, arkoses, metagraywackes and quartzites may be attributable to Ordovician age whereas marbles, black shales, and calc-schists may be considered of Silurian age.

In central and northern Sardinia several granitoid plutons crop out over about 6000 km^2. The sequence of intrusive events linked to the Hercynian orogeny evolve towards more silicic compositions. These events can be distinguished as two main phases: (I) a sin-late tectonic regime (from gabbro-tonalitic to monzogranitic rocks) and (II) a post-tectonic regime (leucogranites) (Bralia *et al.*, 1982). Radiometric estimations indicate mainly granitoid facies with ages ranging from 310 to 290 Ma (Del Moro *et al.*, 1975). The Hercynian granitoid rocks of the investigated area are mainly represented by granodiorites (Ghezzo and Orsini, 1982), locally characterized by pegmatitic and microgranitic facies. Granodiorites are the host rocks of the albitites. The albitites, generally vein-shaped bodies, are widespread in the investigated area and mainly occur at the points where faults cross. Frequently they are mined as a source of feldspar. Their origin is commonly attributed to later Hercynian metasomatic processes mainly involving K-depletion, dissolution of quartz and Na-enrichment under conditions of a positive thermal gradient (Bornioli *et al.*, 1993, Fiori *et al.*, 1994; Bornioli *et al.*, 1996).

During the Tertiary an important tectonic activity affected the Palaeozoic basement of Sardinia and brougth about rifting and formation of a north-south complex graben structure, on the western side of the island. This volcanism has a calcalkaline s.l.

character and is widely considered to be related to a NW or NNW dipping subduction zone along the Paleo-European margin, with consequent drift and counterclockwise rotation of the Sardinia-Corsica microplate. The volcanic activity started about 32 Ma and ended about 13–11 Ma. The volcanics consist of recurrent andesitic suites (andesites associated with minor amounts of basalts, dacites and rhyolites) and ignimbritic suites (of prevalently rhyolitic to dacitic composition, mainly represented by ash and pumice flows and/or falls, with minor lava flows) (Beccaluva *et al.*, 1989). In the investigated area the volcanic formations consist of strongly welded ignimbrites with intercalated cineritic and sedimentary tuffs.

Quaternary slope and alluvial sediments only occur in the area near Ottana. The main structural features in the investigated area are a later Hercynian fault system often reactivated by the Alpine tectonics (Oligocene-Aquitanian). The regional NE-SW fault of Ottana crosses the study area. The general trend is characterized by NE-SW and NW-SE faults; this structural arrangement exhibits a series of blocks, horizontally and perpendicularly shifted with respect to the main faults.

Petrography

The granodiorite. The rock relates to the late-Hercynian magmatism of Sardinia. The petrographic study confirms that the granitoid complex ranges from granodiorite to biotite granodiorite. It is a medium-grained rock, frequently affected by a marked textural anisotropy, probably originated from the tectonics (Ghezzo and Orsini, 1982). The main primary minerals are quartz, generally occurring in small or medium anhedral crystals; plagioclase, varying from oligoclase (An_{20}–An_{28}) to andesine (An_{31}–An_{38}); these occur in subhedral and euhedral crystals, frequently zoned with anorthitic core and albitic rim; K-feldspar is a microcline and occurs in anhedral microperthitic crystals and, finally, biotite occurs in small or medium euhedral crystals, frequently altered to chlorite. The main accessory minerals are: allanite, generally metamict and occurring in medium subhedral or euhedral crystals, frequently zoned; zircon, occurring in small anhedral crystals; and titanite, frequently associated with biotite and occurring in subhedral crystals.

The albitites. Field investigations and petrographic studies suggest that the mineralization originated through a metasomatic alteration of granodiorites: albitization, silicification and chloritization, the most important alteration evidences, support this hypothesis. The metasomatic effects are localized near the faults especially where faults cross. The transition from albitite to unaltered rock is seldom well defined, almost always gradational and in this case limited to a few metres. The main mineral phases are albitic plagioclase, up to 70% in modal proportion, quartz and K-feldspar. Accessory minerals are, besides allanite and epidote, chlorite, titanite and muscovite. The albite frequently occurs in large or medium euhedral crystals and overprints K-feldspar, a more calcic-plagioclase or infilling secondary fractures. Quartz generally occurs in small-to-medium anhedral crystals; K-feldspar occurs as microperthitic subhedral or anhedral microcline. Chlorite is the main mineral of the accessory assemblage; it often overprints or partially replaces biotite along the rim or cleavage. Titanite occurs in subhedral crystals and it is frequently associated with the biotite. Epidote occurs in anhedral crystals. It frequently crystallizes in vugs and veinlets including quartz and plagioclase relics. Muscovite rarely occurs within albitites and generally overprints K-feldspar, biotite and plagioclase.

Experimental

The albitite sampling area is schematically described in Fig. 1; over one hundred samples were collected across the mineralized zones and studied using electron microprobe techniques. The mineral assemblages and *REE*-bearing minerals within the albitites were determined by wavelength dispersive electron probe microanalysis using an A.R.L. microprobe. Analyses were performed at an accelerating voltage of 20 kV and a beam current of approximately 20 nA. Absolute abundances for *REE* were determined by comparison of X-ray count data with synthetic glass standards doped with *REE*. Reference minerals were anorthite for Ca, albite for Si, Al, Na, ilmenite for Ti, Fe, olivine for Mg, thorianite for Th, microcline for K. Raw data were corrected by the ZAF procedure using the Magic IV program.

The following mineral chemistry only refers to the main albitite minerals (K-feldspar, plagioclase) and to the most important accessory ones (chlorite and *REE*-bearing minerals).

Mineral chemistry

Plagioclase and K-feldspar. The chemical composition for the plagioclase feldpsars are reported in Table 1 (see P_1 and P_2 analyses). As can be seen they range from albite to oligoclase. The representative analysis for K-feldspar is also reported in Table 1. *REE* were not detected.

Chlorite. Table 2 shows three representative analyses showing the chemical compositional variation for the chlorites. *REE* were not detected.

Titanite. Titanite analyses have been recalculated using the charge balance criterion of 12 cations per 32 negative charges. The total content of (*REE*+Y),

TABLE 1. Plagioclase and K-feldspar microprobe analyses

	P_1	P_2	K
SiO_2	67.33	65.89	64.22
TiO_2	0.23	0.02	0.01
Al_2O_3	19.63	21.36	18.37
FeO	0.19	–	0.03
CaO	0.46	2.41	–
Na_2O	11.98	10.24	0.29
K_2O	0.02	0.04	16.67
Total	99.84	99.98	99.59
Numbers of ions on the basis of 32(O)			
Si	11.84	11.58	11.96
Ti	0.03	–	–
Al	4.07	4.42	4.03
Fe^{2+}	0.03	–	–
Ca	0.09	0.45	–
Na	4.08	3.49	0.10
K	–	0.01	3.96
Cations	20.14	19.95	20.05
Ab	97.82	88.29	2.58
An	2.07	11.48	–
Or	0.11	0.23	97.42

P_1 = albite; P_2 = oligoclase; K = microcline.

TABLE 2. Chlorite microprobe analyses

	CHL_1	CHL_2	CHL_3
SiO_2	25.46	31.15	27.51
TiO_2	0.02	0.06	–
Al_2O_3	21.51	20.92	22.75
Fe_2O_3	0.00	0.00	1.33
FeO	24.56	19.07	8.81
MnO	0.18	0.15	0.08
MgO	14.43	13.77	27.32
CaO	0.11	0.43	0.05
Na_2O	–	–	–
K_2O	0.04	0.78	–
H_2O*	11.47	11.54	12.38
Total	97.78	97.87	100.24
Numbers of ions on the basis of 28 (O)			
Si	5.464	6.634	5.314
Al^{IV}	2.536	1.366	2.686
Al^{VI}	2.904	3.884	2.492
Ti	0.004	0.010	0.000
Fe^{3+}	0.000	0.000	0.194
Fe^{2+}	4.408	3.396	1.424
Mn	0.032	0.028	0.014
Mg	4.616	4.372	7.866
Ca	0.026	0.098	0.010
Na	0.000	0.000	0.000
K	0.010	0.212	0.000
(OH)	16.000	16.000	16.000
Cations	20.000	20.000	20.000

* calculated by MINFILE program (Afifi and Essene, 1988)

in two representative analyses of *REE*-enriched titanites, ranges from 0.021 and 0.174 a.f.u. (atoms per formula unit); the titanites in the granodiorites are instead always *REE*-free (Table 3). The titanites are preferentially *HREE*-enriched. Figure 2 shows the field of chondrite-normalized *REE* profiles for *HREE*-rich titanites in albitites.

The mechanism of element substitutions (Table 3) occurs in the following scheme, involving Fe^{3+} and Al:

$$Ca^{2+} + Ti^{4+} \rightarrow (REE + Y)^{3+} + (Al, Fe)^{3+} \quad (1)$$

(Green and Pearson, 1986).

Epidote-group minerals. The epidote-group formulae have been based on the structure refinement of Dollase (1971) with the general formula:

$$A_2\, M_3\, Si_3\, O_{12}\, (OH) \quad (2)$$

A sites contain high coordination number cations (Ca, Sr, Lanthanides, etc.). *M* sites are occupied by octahedrally coordinated, trivalent (occasionally divalent) cations such as Al, Fe^{3+}, Mn^{3+}, Fe^{2+}, Mg, etc. More particularly, the epidote-group formula may be represented as:

$$\begin{array}{ccccccc} (A_1) & (A_2) & & (M_1) & (M_2) & (M_3) & \quad (3) \\ \downarrow & \downarrow & & \downarrow & \downarrow & \downarrow & \\ Ca_1 & (Ca_{1-x}REE_x) & & (Al_{1-y}Fe^{3+}_y) & Al_1 & (Al_{1-z}Fe^{2+}_z)Si_3O_{12}(OH) & \end{array}$$

Allanite appears to form a complete solid solution with the $FeAl_2$-epidote end-member species through the coupled substitution (Maaskant *et al.*, 1980; Sakai *et al.*, 1984; Deer *et al.*, 1986; Gieré, 1986; Pan and Fleet, 1990):

$$Ca_{A2} + Fe^{3+}_{M1} = REE_{A2} + Fe^{2+}_{M3} \quad (4)$$

By definition (Pan and Fleet, 1991) allanite requires at least 50% occupancy of the A_2 site by total rare earth elements (*REE*) corresponding to 15 wt.%. In the granodiorites a metamict and zoned allanite has been recorded; it generally appears in prismatic crystals and displays a distinct pale green colour in plane-polarized light. Microprobe analyses show that ThO_2 is preferentially concentrated at the crystal rims; its content is higher than in the allanites

TABLE 3. Titanite microprobe analyses

	T_1	T_2	T_3
SiO_2	29.34	29.43	29.32
TiO_2	34.27	37.73	34.63
Al_2O_3	2.74	1.63	2.90
FeO	0.13	0.12	0.76
MnO	–	–	0.14
MgO	0.01	–	–
CaO	27.10	28.34	28.37
Na_2O	0.02	–	–
Y_2O_3	1.57	0.11	0.07
La_2O_3	–	–	–
Ce_2O_3	0.24	0.08	–
Pr_2O_3	–	–	–
Nd_2O_3	0.44	0.18	–
Sm_2O_3	0.29	–	–
Gd_2O_3	0.34	–	–
Total	96.49	97.62	96.19
Numbers of ions on the basis of 16 (O)			
Si	3.963	3.909	3.911
Ti	3.481	3.769	3.473
Al	0.436	0.255	0.457
Fe^{2+}	0.015	0.013	0.085
Mn	–	–	0.016
Mg	0.002	–	–
Ca	3.922	4.033	4.053
Na	0.005	–	–
Y^{3+}	0.113	0.008	0.005
Sum (*REE*)	0.061	0.013	–
Ca site	4.101	4.054	4.074
Ti site	3.897	3.946	3.926
Cations	12.000	12.000	12.000

T_1, T_2 = titanites in albitite
T_3 = titanite in granodiorite

of albitites (Fig. 3). *REE*-rich epidote is never found. Detailed SEM investigations show that the albitite epidotes prevalently occur in subhedral and anhedral crystals. They frequently replace primary minerals (generally plagioclase and magmatic allanite, rarely quartz) and infill vugs and veinlets. Allanite is commonly recorded in close association with *REE*-rich epidotes. A frequent compositional zonation (see Exley, 1980) was observed using the backscattered electron (BSE) technique (Lloyd, 1987). The patchy zones are attributable to the variation in *LREE* contents. Using a grey scale mode the content of *LREE* is higher in the lighter than in the darker zones. Figures 4 and 5 show the patchy zoning in epidotes:

I. an epidote-(Ce) crystal leached by metasomatic fluids complexing and mobilizing *REE* (Fig. 4);

II. a *LREE*-free epidote crystal *REE*-enriched by the mobilized *REE* (see Fig. 5).

It may be assumed that these situations correspond to a complex mechanism of *REE* mobilization by leaching from minor mineral phases and selective accommodation in epidote with fluids restricted and channelled or pervasive. On this subject the presence of *LREE*-rich epidotes infilling fractures and vugs and patchy epidote-(Ce) is fairly frequent. But, on the other hand, it is not easy to ascertain which of situations I and II is more frequent because of a progressive and local modification of fluid characteristics, porosity and reactivity of precursor granitoid that could have influenced possible gain or loss of *LREE* during the alteration process. On this subject, Fig. 2 shows the range of the chondrite normalized *REE*-profiles for the analyses of Table 4. Therefore, the similarity of patterns suggests that epidotes developed from hydrothermal fluids with the same chemical characteristics. But, on the other hand, a progressive change in *LREE* content of fluids and local changes in permeability and porosity of the precursor granitoid could have influenced the interaction between fluids and rocks.

Table 5 summarizes four representative analyses (cross-referenced on Fig. 4) of epidote and allanite-(Ce); they are plotted in the Al^{3+}–Fe^{3+} diagram (Fig. 6), with Fe^{3+} calculated on a stoichiometric basis according to Droop (1987).

Figure 7 shows the inverse correlation $\Sigma LREE$ + Fe^{2+} + Mg+ Mn *vs.* Ca + Al^{3+} + Fe^{3+} caused by substituting divalent for trivalent species, according to Eqn. (4). Figure 7 also shows the complete solid solution existing between allanite and other epidote-group minerals. The maximum total *REE* content attains up to 22 wt.%. Figure 8 shows the distribution of the most abundant *LREE* (Ce_2O_3, La_2O_3, Nd_2O_3) in *REE*-rich epidotes and allanites.

The Ps parameter (= $Fe^{3+}/(Fe^{3+}$ + Al)) (Tulloch, 1979, 1986; Vyhnal *et al.*, 1991) is also included in Table 4. This chemical criterion, proposed by Tulloch (1979) for recognizing magmatic epidote in granitic rocks, demonstrates that epidotes formed from alteration of plagioclase ranged from Ps_0 to Ps_{24}, those formed by alteration of biotite from Ps_{36} to Ps_{48} and those exhibiting magmatic texture from Ps_{25} to Ps_{29}. The above criterion confirms the results obtained by the SEM textural study: the epidotes originated mainly from plagioclase alteration and magmatic allanite; only a few crystals are of presumed magmatic origin and inherited from the granodiorites.

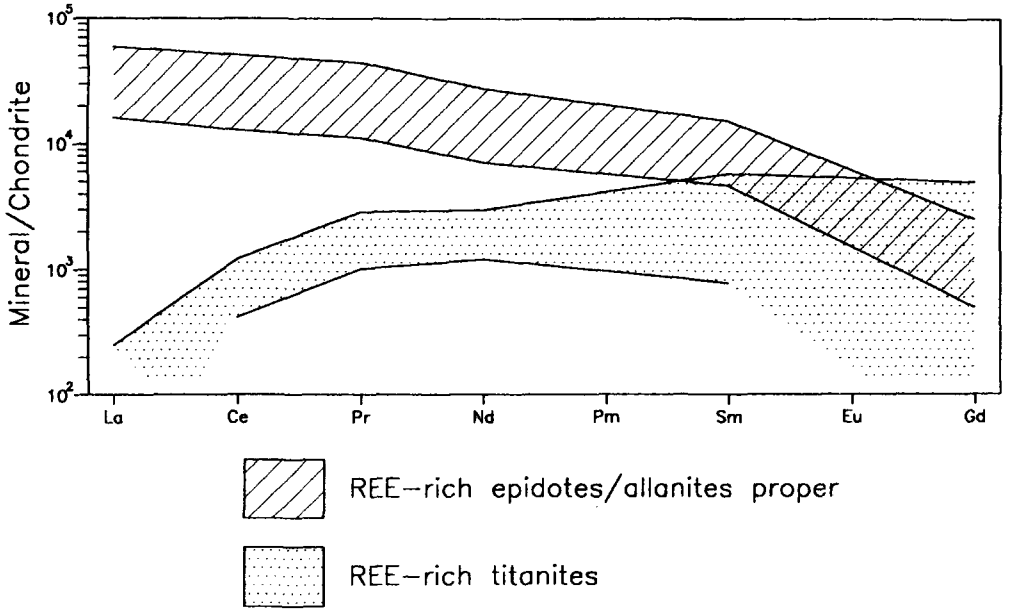

FIG. 2. Field of chondrite-normalized *REE* profiles for *REE*-rich titanites, *REE*-rich epidotes and allanites in albitites, from microprobe data.

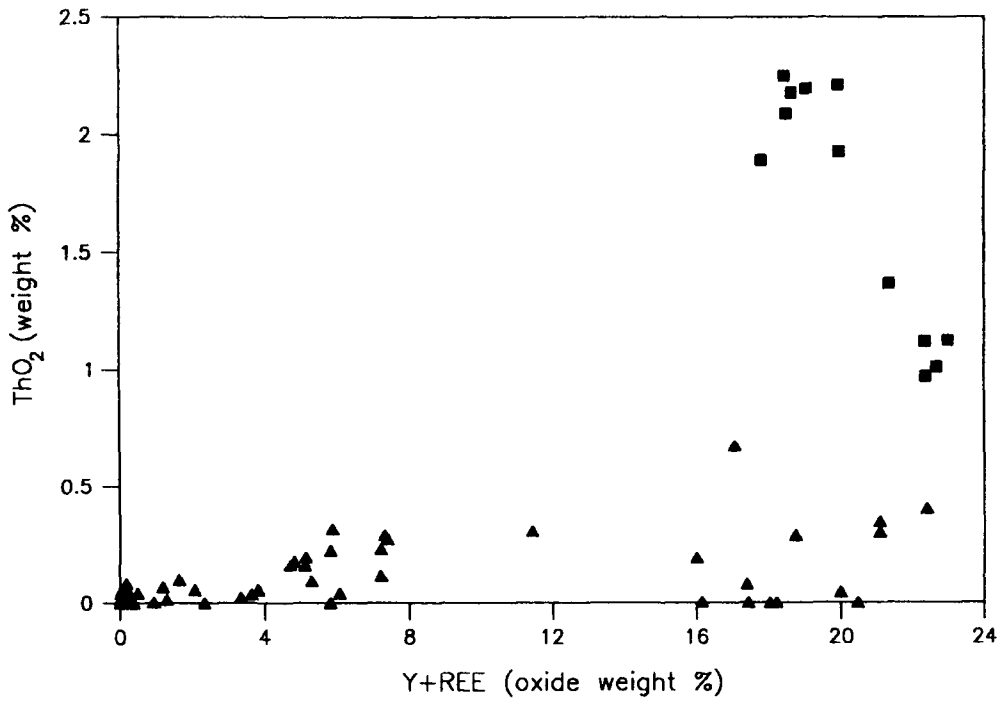

FIG. 3. Total *REE*+Y *vs.* ThO_2 variation diagram for epidotes and allanites of granodiorites and albitites, from microprobe data. Solid squares — granodiorites; triangles — albitites.

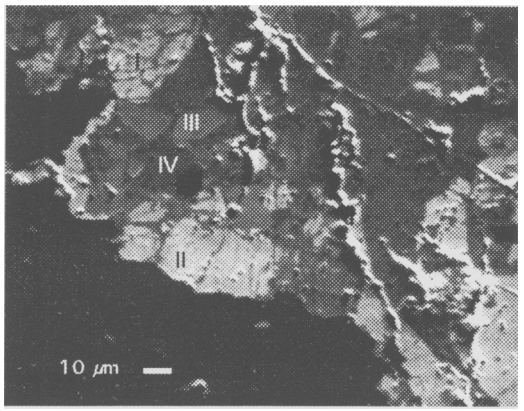

FIG. 4. Typical patchy-zoned epidote in albitite. Back scattered electron image. For chemical composition of (I), (II), (III) , (IV) zones, see Table 5.

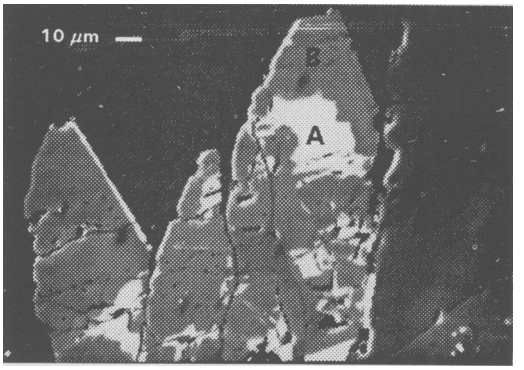

FIG. 5. Allanite (*A*) and *REE*-rich epidote (*B*) in an epidote crystal in albitite. Back scattered electron image.

Discussion

As regards the model explaining the origin of the albitites the reader is referred to Bornioli *et al.* (1993). According to these authors, the origin of the albitites may be attributed to the metasomatic alteration that affected the granodiorites, caused by the circulation of later Cl-enriched fluids in fractures and faults of the granitoids. The mineralogic and petrographic studies show that mineral composition gradually changes from the unaltered rock to the most altered zone; albite, chlorite, epidote (the latter more or less *LREE*-enriched) as well as quartz and more rare muscovite and K-feldspar, are the authigenic minerals but their concentration and occurrence vary from one zone to another.

The replacement of the most important magmatic minerals can be schematized as follows:

K-feldspar → ↗ K-feldspar / muscovite / ↘ albite

oligoclase → ↗ albite / ↘ epidote

biotite → ↗ titanite / epidote / ↘ chlorite

allanite → ↗ epidote / ↘ *LREE*-rich epidote

The *REE* mobilization and their strong fractionation (unaltered rocks: $16< (La/Lu)_n <49$; albitites: $18< (La/Lu)_n <96$) (Bornioli *et al.*, in press), the distribution of *HREE* in the titanites and *LREE* in epidotes are considerations that improve the hypotheses about a metasomatic alteration involving Cl-bearing fluids (Fiori *et al.*, 1994). In fact, under certain conditions the *REE* are highly mobile at elevated temperatures, particularly in hydrothermal systems. Mobility of the *REE* is largely dependent on the nature of the original *REE*-bearing mineral phases, composition of the fluid phase and ability of minerals formed during the reactions to accommodate the *REE* from the fluid (Humphris, 1984). *REE* fractionation may occur during fluid transport owing to selective mobility of the *REE* or by selective accommodation in newly-formed minerals. The solubility and liquid–solid distribution coefficients of *REE* are greatly increased by the presence of ligands in solution. The complexing agents such as F, Cl and CO_2 appear to be the main parameters in controlling the *REE* behaviour and their fractionation. Experiments with Cl complexing show preferential mobilization of *LREE* and Eu (Flynn and Burnham, 1978; Taylor and Fries, 1983); the complexing by either F or CO_2 has been advocated to explain preferential mobilization of *HREE* (Balashov and Kriegman, 1975; Campbell *et al.*, 1984). Semenov (1958) attributed the preference for *LREE* accommodation to a crystal-chemical control. He showed that mineral structures having a cation site with high cationic coordination sites prefer the *HREE* (titanite). Allanite, which has an 11-fold-coordinated site (Dollase, 1971), would therefore be expected to contain a large proportion of *LREE*. During the hydrothermal phase it is conceivable that *REE* were mobilized by leaching from minor mineral

TABLE 4. *REE*-rich epidote and allanite proper representative analyses

Sample	1	2	3	4	5	6	7	8	9	10	11	12	13	14	15	16	17	18	19	20
SiO_2	31.81	31.64	30.41	31.06	33.99	32.94	31.95	32.64	34.88	39.67	35.59	35.75	34.94	37.17	36.17	35.87	36.16	36.37	35.08	35.87
TiO_2	0.08	0.50	0.04	0.08	0.10	0.04	0.02	0.02	0.05	0.10	0.01	0.02	0.02	0.20	0.02	0.03	0.08	0.03	0.03	0.04
Al_2O_3	21.43	16.20	21.39	22.67	21.61	22.85	21.05	23.65	23.77	25.76	23.49	23.07	24.12	25.13	23.62	23.07	23.48	24.44	23.41	23.40
FeO*	9.02	15.52	7.32	7.68	8.37	7.91	8.51	7.61	8.49	7.24	11.24	11.20	10.33	10.13	10.68	10.67	10.33	8.96	10.85	9.21
MnO	–	0.40	–	0.06	–	0.07	–	–	–	–	0.02	0.04	0.02	0.02	–	0.01	0.01	0.17	0.03	0.05
MgO	0.10	0.02	1.31	0.08	0.20	0.10	0.97	0.37	0.09	0.30	0.14	0.15	0.16	0.10	0.03	0.03	0.10	0.05	0.11	0.14
CaO	13.56	11.52	13.88	14.62	15.30	15.16	14.68	15.25	18.02	19.86	19.73	19.80	19.49	22.47	20.58	20.28	20.47	20.81	20.13	20.84
La_2O_3	3.40	4.43	5.08	2.80	4.54	3.21	4.78	4.82	2.68	1.65	1.79	1.80	1.72	0.90	1.11	1.33	1.35	1.34	1.12	1.43
Ce_2O_3	10.96	9.66	9.30	9.22	9.20	9.09	7.75	7.04	5.41	3.75	3.69	3.60	3.58	3.48	2.79	2.78	2.74	2.68	2.37	2.35
Pr_2O_3	1.19	1.16	0.98	1.10	0.79	1.02	0.90	0.64	0.60	0.40	0.28	0.37	0.36	–	0.30	0.30	0.08	0.35	0.28	0.24
Nd_2O_3	4.08	5.15	3.81	3.93	3.46	3.32	3.16	2.59	2.25	1.13	1.24	1.27	1.37	0.14	1.21	1.15	0.96	1.15	1.15	0.90
Sm_2O_3	0.67	1.08	0.63	0.78	0.65	0.69	0.42	0.49	0.42	0.14	0.17	0.22	0.13	0.12	0.22	0.25	0.14	0.17	0.15	0.16
Gd_2O_3	–	0.41	0.12	0.27	–	–	–	0.16	–	–	–	–	–	–	0.12	–	–	–	–	–
Y_2O_3	0.07	0.52	0.08	0.14	0.06	0.07	–	0.27	0.04	0.05	0.03	0.07	0.06	–	0.06	0.03	0.02	0.05	0.05	0.03
ThO_2	–	0.40	–	–	0.29	–	0.67	0.19	0.31	0.12	0.23	0.27	0.29	0.16	0.22	0.32	0.09	–	0.20	0.16
Total	96.37	98.61	94.35	94.49	98.56	96.47	94.86	95.74	97.01	100.17	97.65	97.63	96.59	100.02	97.13	96.12	96.01	96.57	94.96	94.82
Numbers of ions on the basis of 12.5 (O)																				
Si	2.932	2.974	2.832	2.865	3.017	2.950	2.923	2.911	2.978	3.157	2.943	2.962	2.916	2.932	2.976	2.989	2.995	2.990	2.940	2.999
Ti	0.006	0.035	0.003	0.005	0.007	0.002	0.001	0.001	0.003	0.006	–	0.001	0.002	0.012	0.001	0.002	0.005	0.002	0.002	0.002
Al^{IV}	0.068	0.026	0.168	0.135	–	0.050	0.077	0.089	0.022	–	0.057	0.038	0.084	0.068	0.024	0.011	0.005	0.010	0.060	0.001
Al^{VI}	2.261	1.769	2.181	2.330	2.262	2.363	2.195	2.398	2.370	2.417	2.233	2.216	2.288	2.270	2.268	2.256	2.288	2.359	2.253	2.306
Fe^{3+} †	0.110	0.398	0.302	0.182	0.073	0.113	0.285	0.157	0.279	0.046	0.596	0.587	0.562	0.634	0.571	0.563	0.544	0.475	0.638	0.528
Fe^{2+}	0.585	0.822	0.268	0.410	0.549	0.480	0.367	0.410	0.328	0.436	0.181	0.189	0.159	0.034	0.164	0.181	0.172	0.141	0.122	0.116
Mn	–	0.032	–	0.005	–	0.005	–	–	–	–	0.001	0.003	0.001	0.002	–	0.001	–	0.012	0.002	0.003
Mg	0.013	0.003	0.182	0.010	0.027	0.013	0.132	0.049	0.012	0.036	0.017	0.019	0.020	0.012	0.004	0.004	0.013	0.007	0.014	0.018
Sum(M)	3.043	3.085	3.104	3.077	2.918	3.026	3.057	3.104	3.014	2.941	3.085	3.053	3.116	3.032	3.032	3.018	3.027	3.006	3.091	2.974
Ca	1.339	1.160	1.385	1.445	1.455	1.455	1.440	1.457	1.648	1.693	1.748	1.758	1.742	1.900	1.814	1.811	1.816	1.833	1.808	1.867
Y	0.004	0.026	0.004	0.007	0.003	0.003	–	0.013	0.002	0.002	0.001	0.003	0.002	–	0.003	0.001	0.001	0.002	0.002	0.001
Th	–	0.009	–	–	0.006	–	0.014	0.004	0.006	0.002	0.004	0.005	0.005	0.003	0.004	0.006	0.002	–	0.004	0.003
Sum (*REE*)	0.681	0.746	0.676	0.606	0.603	0.565	0.567	0.511	0.353	0.205	0.216	0.219	0.218	0.134	0.172	0.176	0.159	0.170	0.155	0.155
Sum(A)	2.024	1.941	2.065	2.058	2.067	2.023	2.021	1.985	2.009	1.902	1.969	1.985	1.967	2.037	1.993	1.994	1.978	2.005	1.969	2.026
PS	5	18	11	7	3	4	11	6	10	2	21	21	19	21	20	20	19	17	22	19

TABLE 4 (*contd*)

Sample	21	22	23	24	25	26	27	28	29	30	31	32	33	34	35	36	37
SiO_2	34.83	36.39	36.61	36.80	36.17	37.70	38.26	35.97	37.31	38.14	38.04	36.82	38.14	38.03	38.12	37.08	37.02
TiO_2	0.02	0.03	0.16	0.08	0.03	0.01	0.10	0.02	0.05	0.18	0.03	0.10	0.02	–	0.03	0.31	0.04
Al_2O_3	23.46	26.17	27.23	26.29	25.65	25.74	26.62	24.05	25.65	29.82	28.78	23.23	33.20	30.51	31.47	23.26	23.86
FeO*	10.77	7.39	5.89	6.19	7.21	10.06	8.80	8.31	9.24	4.62	6.83	12.92	1.19	5.14	3.53	12.69	12.32
MnO	0.02	–	0.01	0.01	0.01	0.23	0.17	0.03	0.29	0.02	0.04	0.13	0.01	0.02	0.05	0.04	0.05
MgO	0.10	0.21	0.22	0.20	0.11	0.02	0.01	0.03	0.03	0.02	–	–	–	–	0.02	–	–
CaO	21.11	21.88	21.83	21.88	21.94	22.76	23.24	21.89	22.65	23.14	23.63	22.91	23.79	23.82	23.93	23.39	23.21
La_2O_3	1.20	1.01	0.74	1.14	0.56	0.59	0.26	0.61	0.13	0.52	0.08	0.15	–	–	–	–	–
Ce_2O_3	2.30	1.83	1.61	1.45	1.19	0.70	0.68	0.64	0.33	0.29	0.24	0.15	0.12	0.10	–	–	–
Pr_2O_3	0.24	0.08	0.18	–	–	–	–	0.19	0.08	0.11	–	–	–	–	–	–	–
Nd_2O_3	0.80	0.73	0.77	0.43	0.38	0.17	0.20	0.44	0.26	0.16	0.11	–	–	–	–	–	–
Sm_2O_3	0.15	0.13	0.12	0.18	0.11	0.05	–	0.06	–	0.05	–	–	–	–	–	–	–
Gd_2O_3	–	–	0.10	–	–	–	–	0.11	–	–	–	–	–	–	–	–	–
Y_2O_3	0.09	–	0.11	0.08	0.04	0.05	0.03	–	0.06	–	–	–	–	–	–	–	–
ThO_2	0.18	0.06	–	–	–	0.10	–	0.06	–	0.07	–	–	–	–	–	–	0.05
Total	95.27	95.91	95.58	94.73	93.40	98.18	98.37	92.41	96.08	97.14	97.78	96.41	96.47	97.62	97.15	96.77	96.55
Numbers of ions on the basis of 12.5 (O)																	
Si	2.899	2.953	2.964	3.004	2.984	2.966	2.984	3.011	2.979	2.975	2.948	2.950	2.939	2.929	2.935	2.953	2.949
Ti	0.002	0.002	0.010	0.005	0.002	0.001	0.006	0.001	0.003	0.011	0.002	0.006	0.001	–	0.001	0.019	0.002
Al^{IV}	0.101	0.047	0.036	–	0.016	0.034	0.016	–	0.021	0.025	0.052	0.050	0.061	0.071	0.065	0.047	0.051
Al^{VI}	2.202	2.457	2.563	2.530	2.478	2.354	2.432	2.374	2.393	2.717	2.578	2.144	2.954	2.699	2.791	2.137	2.191
Fe^{+3} †	0.743	0.473	0.346	0.352	0.466	0.630	0.539	0.538	0.596	0.252	0.457	0.885	0.102	0.369	0.271	0.873	0.853
Fe^{+2}	0.007	0.028	0.053	0.071	0.032	0.032	0.035	0.044	0.021	0.050	–	–	–	–	–	–	–
Mn	0.001	–	–	0.001	0.001	0.015	0.011	0.002	0.020	0.001	0.002	0.009	0.001	0.001	0.003	0.003	0.003
Mg	0.013	0.025	0.027	0.024	0.014	0.002	0.001	0.003	0.003	0.002	–	–	–	–	0.002	–	–
Sum(M)	3.069	3.032	3.035	2.983	3.009	3.068	3.040	2.962	3.057	3.058	3.091	3.094	3.119	3.140	3.133	3.079	3.100
Ca	1.883	1.902	1.894	1.914	1.939	1.919	1.943	1.963	1.938	1.934	1.962	1.967	1.964	1.966	1.974	1.996	1.982
Y	0.004	–	0.005	0.004	0.002	0.002	0.001	–	0.003	–	–	–	–	–	–	–	–
Th	0.003	0.001	–	–	–	0.002	–	0.001	–	0.001	–	–	–	–	–	–	0.001
Sum (*REE*)	0.142	0.112	0.103	0.096	0.067	0.044	0.032	0.062	0.023	0.032	0.012	0.009	0.003	0.003	–	–	–
Sum(A)	2.032	2.015	2.002	2.014	2.008	1.967	1.976	2.026	1.964	1.967	1.974	1.976	1.967	1.969	1.974	1.996	1.983
PS	24	16	12	12	16	21	18	18	20	8	15	29	3	12	9	29	28

* Total iron as FeO. PS = pistacite wt.%. – = not detectable

† Calculated on a stoichiometric basis according to Droop (1987)

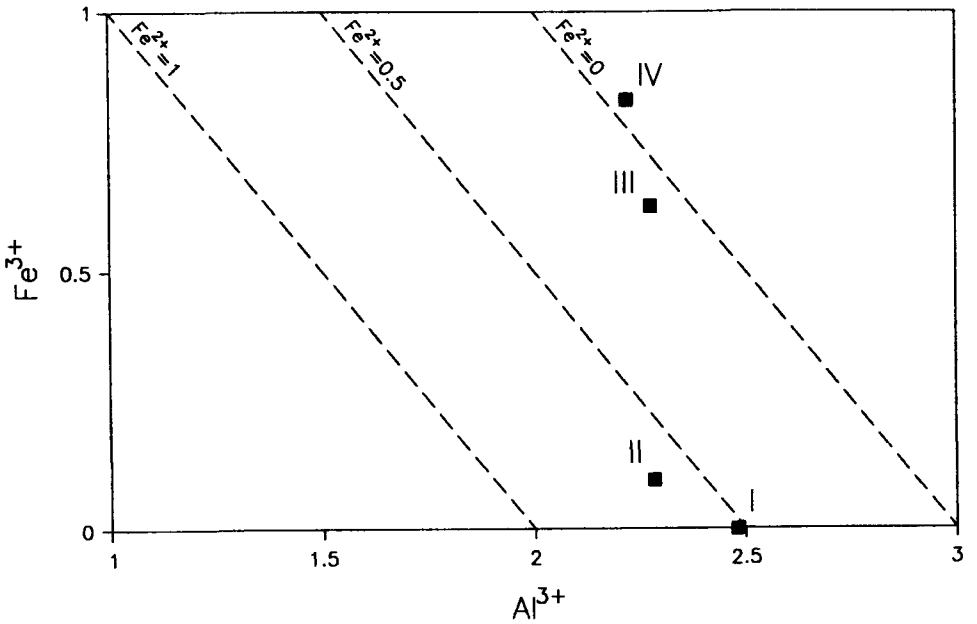

FIG. 6. Variation in a.f.u. $Fe^{3+}-Al^{3+}$composition of allanites and epidotes in the albitites, from microprobe data (see Table 5).

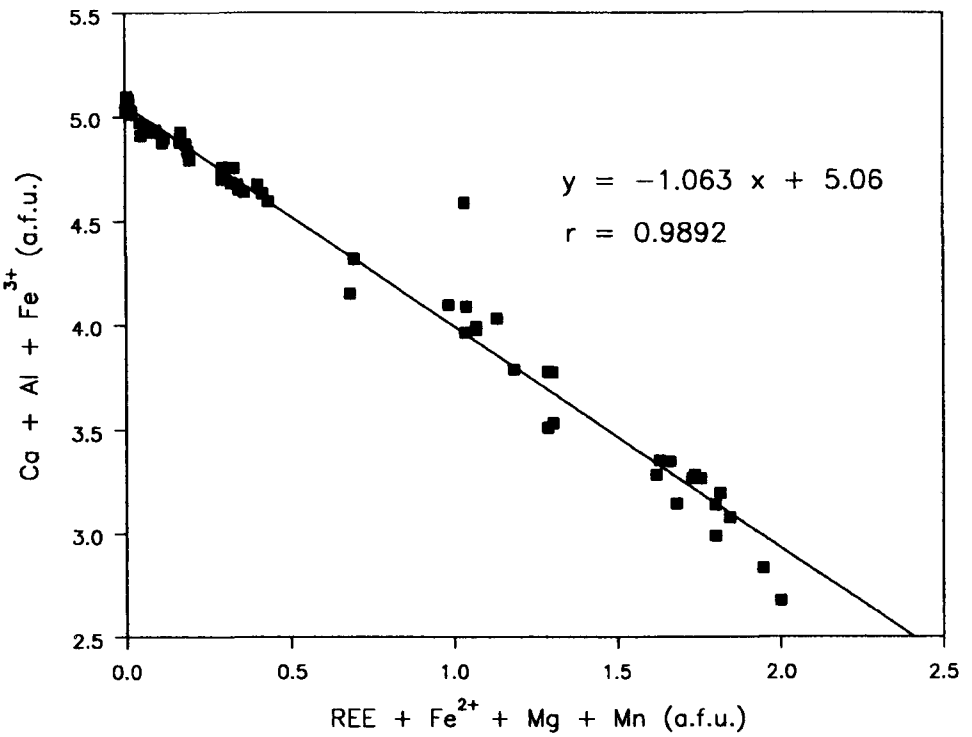

FIG. 7. $\Sigma LREE$ + Fe^{2+} + Mg + Mn *vs.* Ca + $Al^{3+}Fe^{3+}$ diagram for epidotes, from microprobe data.

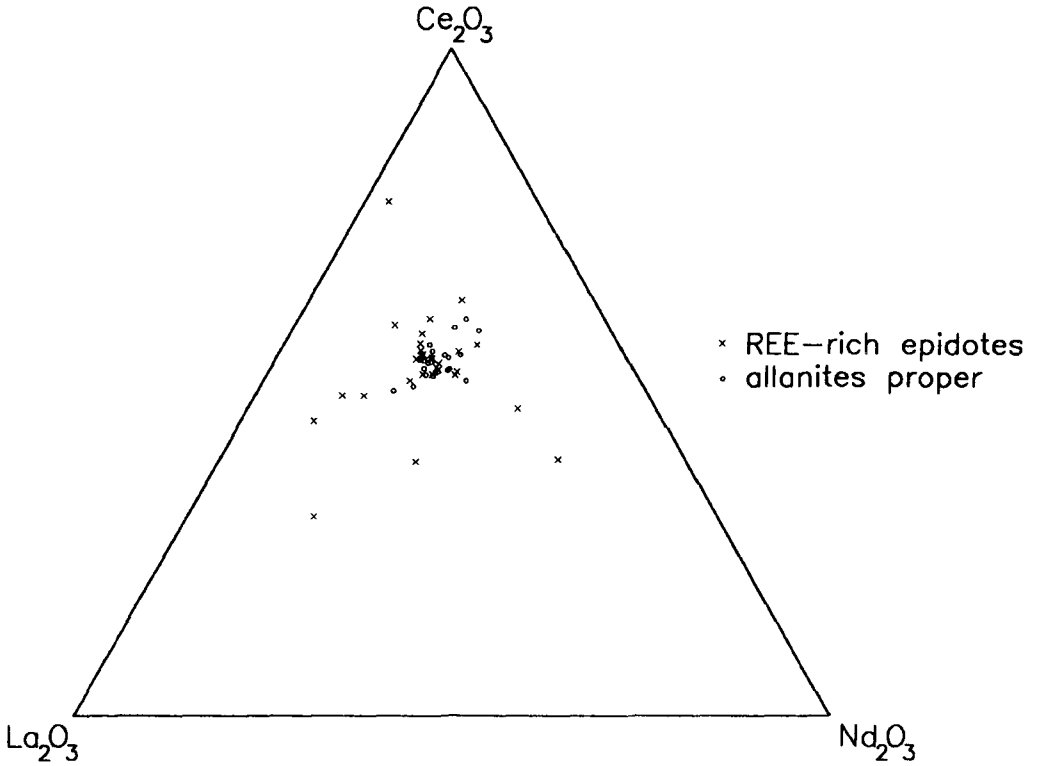

FIG. 8. Ce_2O_3–Nd_2O_3–La_2O_3 diagram for *REE*-rich epidotes and allanites in albitite, from microprobe data.

phases (essentially allanite) in the granodiorite and were selectively accommodated in newly-formed epidotes. It may be assumed that the textural differences observed in epidotes correspond to a complex mechanism of *REE* mobilization with fluids resctricted or channelled and pervasive. Combined textural feature study and EPMA analyses indicate that *LREE* are distributed randomly in these minerals also because the hydrothermal fluids progressively changed concentration of *REE* in time (Carcangiu *et al.*, 1993).

The schematic model of the epidote-forming reactions, during the metasomatic processes that affected the granodiorites, involves the instability of the anorthitic component of plagioclase, the simultaneous formation of albite and leaching of the magmatic allanite with a redistribution of *LREE* in the epidotes. The similarity of patterns suggests that epidotes developed from hydrothermal fluids with the same chemical characteristics. But, on the other hand, a progressive change in *LREE* content of fluids and local changes in permeability and porosity of the precursor granitoid could have influenced the interaction between fluids and rocks.

Acknowledgements

This work forms part of the programmes of the 'Centro Studi Geominerari e Mineralurgici' (Cagliari, Italy) of the Consiglio Nazionale delle Ricerche, in the framework of the 'Caratterizzazione e valorizzazione dei minerali contenenti Terre Rare in Sardegna' project.

References

Afifi, A.M. and Essene, E.J. (1988) MINFILE: A microcomputer program for storage and manipulation of chemical data on minerals. *Amer. Mineral.*, **73**, 3–4, 446–8.

Balashov, Y.A. and Kriegman, L.D. (1975) The effects of alkalinity and volatiles on rare earth separation in magmatic systems. *Geochem. Intern.*, **12**, 165–70.

Beccaluva, L., Macciotta, G., Siena, F. and Zeda, O. (1989) Harzburgite - lherzolite xenoliths and clinopyroxene megacrysts of alkaline basic lavas from Sardinia (Italy). *Chem. Geol.*, **77**, 331–45.

Bornioli, R., Carcangiu, G., Palomba, M., Peretti, R., Tamanini, M. and Zucca, A. (1993) *REE*-miner-

TABLE 5. Allanite and epidote representative analyses

	I	II	III	IV
SiO_2	34.96	32.74	35.04	36.25
TiO_2	0.07	0.02	0.01	0.11
Al_2O_3	24.60	22.51	24.15	24.55
FeO	7.22	7.11	10.86	12.38
MnO	–	–	0.02	0.06
MgO	0.16	1.39	0.12	–
CaO	16.02	13.73	19.84	22.67
La_2O_3	3.16	4.52	1.47	–
Ce_2O_3	7.87	10.22	2.80	0.06
Pr_2O_3	0.84	1.10	0.37	–
Nd_2O_3	3.50	4.17	1.19	–
Sm_2O_3	0.52	0.76	0.21	–
Gd_2O_3	0.14	0.18	–	–
Y_2O_3	0.10	0.13	0.04	–
ThO_2	–	0.30	–	–
Total	99.16	98.88	96.12	96.08
Numbers of ions on the basis of 12.5 (O)				
Si	2.996	2.918	2.912	2.905
Ti	0.005	0.001	0.001	0.007
Al^{IV}	0.004	0.082	0.088	0.095
Al^{VI}	2.481	2.283	2.278	2.224
Fe^{3+}	–	0.100	0.625	0.830
Fe^{2+}	0.517	0.430	0.130	–
Mn	–	–	0.001	0.004
Mg	0.021	0.184	0.015	–
Sum (*M*)	3.028	3.079	3.137	3.160
Ca	1.477	1.311	1.767	1.947
Y^{3+}	0.015	0.006	0.002	–
Th^{4+}	0.004	0.006	–	–
Sum (*REE*)	0.485	0.679	0.182	0.002
Sum (*A*)	1.981	2.003	1.951	1.949

(I,II) allanites
(III, IV) epidotes

alization in the albitite deposits of Central Sardinia (Italy). Geological, mineralogical and petrological aspects, *REE*-bearing minerals. Abstracts of Congress *Rare Earth Minerals: Chemistry, Origin and Ore Deposits*, 1-2 April, London, 15–7.

Bornioli, R., Fadda, S., Fiori, M., Grillo, S.M. and Marini, (1996) Genetic aspects of albitite deposit from Central Sardinia: mineralogical and geochemical evidence. *Explor. Mining Geol.*, **5**, 61–72.

Bornioli, R., Carcangiu, G., Palomba, M., Peretti, R., Tamanini, M. and Zucca, A. (in press) Rare earth elements in the albitites of Central Sardinia (Italy). Note I: the mineralization of Ottana.

Bralia, A., Ghezzo, C., Guasparri, G. and Sabatini, G. (1982) Aspetti genetici del batolite sardo-corso. *Rend. Soc. Ital. Mineral. Petr.*, **38**, 701–64.

Campbell, H.I., Lesher, C.M., Coad, P., Franklin, J.M., Gorton, M.P. and Thurston, P.C. (1984) Rare earth elements mobility in alteration pipes below massive Cu-Zn sulfide deposits. *Chem. Geol.*, **45**, 439–87.

Carcangiu, G., Franceschelli, M., Palomba, M. and Tamanini, M. (1993) Allanite-(Ce) and epidotes in a feldspar deposit from Central Sardinia, Italy. Abstracts of Congress *Rare Earth Minerals: Chemistry, Origin, and Ore Deposits*, 1-2 April, London, 23–24.

Deer, W.A., Howie, R.A. and Zussman, J. (1986) *Rock-forming Minerals*, 2nd ed., Vol. 1A., Longmans, London.

Del Moro, A., Di Simplicio, P., Ghezzo, C., Guasparri, G., Rita, F. and Sabatini, G. (1975) Radimetric data and intrusive sequence in the Sardinian Batholith. *Neues Jahrb. Mineral., Abh.*, **126**, 28–44.

Dollase, W.A. (1971) Refinement of the crystal structures of epidote, allanite and hancockite. *Amer. Mineral.*, **56**, 447–64.

Droop, G.T.R. (1987) A general equation for estimating Fe^{3+} concentration in ferromagnesian silicates and oxides from microprobe analyses, using stoichiometric criteria. *Mineral. Mag.*, **51**, 431–5.

Elter, F.M., Franceschelli, M., Ghezzo, C., Memmi, I. and Ricci, C.A. (1986) The geology of Northern Sardinia *Final Meet. of IGCP, May 26-31, Newsletter, special issue,* 87–97.

Exley, R.A. (1980) Microprobe studies of *REE*-rich accessory minerals: implications for Skye granite petrogenesis and *REE* mobility in hydrothermal systems. *Earth Planet. Sci. Lett.*, **48**, 97–110.

Fiori, M., Garbarino, C., Grillo, S.M., Marcello, A., Marini, C. and Pretti, S. (1994) Relazioni genetiche tra le mineralizzazioni ad albite e quelle a clorite-talco della Sardegna centrale. *Atti Conv. 'Giornata di Studio in ricordo di S. Zucchetti'*, 139–45.

Flynn, R.T. and Burnham, C.W. (1978) An experimental determination of rare earth partition coefficients between a chloride containing vapor phase and silicate melts. *Geochim. Cosmochim. Acta*, **42**, 685–701.

Ghezzo, C. and Orsini, J.B. (1982) Lineamenti strutturali e composizionali del batolite ercinico sardo-corso in Sardegna. *Soc. Geol. It., Proceed. Congr. "Geologia del Paleozoico Sardo"*, May 1982, Cagliari, 165–81.

Gieré, R. (1986) Zirconolite, allanite and hoegbomite in a marble skarn from the Bergell contact aureole: implications for mobility of Ti, Zr and *REE*. *Contrib. Mineral. Petrol.*, **93**, 459–70.

Green, T.H. and Pearson, N.J. (1986) Rare earth elements partitioning between sphene and coexisting silicate liquid at high pressure and temperature.

Chem. Geol., **55**, 105–19.

Humphris, S.E. (1984) The *REE* mobility of the rare earth elements in crust. In: *Rare Earth Element Geochemistry* (P. Henderson, Ed.), Elsevier, Amsterdam, 317–42.

Lloyd, G.E. (1987) Atomic number and cristallographic contrast images with the SEM: a review of back-scattered electron techniques. *Mineral. Mag.*, **51**, 3–19.

Maaskant, P., Coolen, J.J.M.M.M. and Burke, E.A.J. (1980) Hibonite and coexisting zoisite and clinozoisite in a calc-silicate granulite from southern Tanzania. *Mineral. Mag.*, **43**, 995–1003.

Pan, Y. and Fleet, M.E. (1990) Halogen-bearing allanite from the White River gold occurrence, Hemlo area, Ontario. *Canad. Mineral.*, **28**, 67–75.

Pan, Y. and Fleet, M.E. (1991) Vanadian allanite-(La) and vanadian allanite-(Ce) from the Hemlo gold deposit, Ontario, Canada. *Mineral. Mag.*, **55**, 497–507.

Sakai, C., Higashino, T. and Enami, M. (1984) *REE*-bearing epidote from Sanbagawa pelitic schists, Central Shikoku, Japan. *Geochem. J.*, **18**, 45–53.

Semenov, E.I. (1958) Relationship between composition of rare earths and composition and structures of minerals. *Geochem.*, **53**, 574–86.

Taylor, R.P. and Fries, B.J. (1983) Rare earth elements lithogeochemistry of granitoid mineral deposits. *Carn. Inst. Metall. Bull.*, **76**, 74–84.

Tulloch, A.J. (1979) Secondary Ca-Al silicates as low grade alteration products of granitoid biotite. *Contrib. Mineral. Petrol.*, **69**, 105–17.

Tulloch, A.J. (1986) Comment on 'Implications of magmatic epidote-bearing plutons on crustal evolution in the accreted terraines of north-western North America' and 'Magmatic epidote and its petrologic significance'. *Geol.*, **14**, 186–7.

Vyhnal, C.R., McSween, H.Y.Jr. and Speer, J.A. (1991) Hornblende chemistry in Southern Appalachian granitoids: implications for aluminium horneblende thermobarometry and magmatic epidote stability. *Amer. Mineral.*, **76**, 176–88.

[*Manuscript received 26 February 1996: revised 31 July 1996*]